Inferring Enterovirus D68 Transmission Dynamics from the Genomic Data of Two 2022 North American outbreaks

Martin Grunnill
Public Health Ontario
Alireza Eshaghi
Public Health Ontario
Lambodhar Damodaran
University of Pennsylvania
Sandeep Nagra
Public Health Ontario
Ali Gharouni
Public Health Ontario
Thomas Braukmann
Public Health Ontario
Shawn Clark
Public Health Ontario
Adriana Peci
Public Health Ontario
Sandra Isabel
Public Health Ontario
Philip Banh
Public Health Ontario
Louis du Plessis
ETH Zurich
Carmen Lia Murall
Public Health Agency of Canada
Caroline Colijn
Simon Fraser University
Samira Mubareka
Sunnybrook Research Institute
Maan Hasso
Public Health Ontario
Justin Bahl

University of Georgia
Heba H. Mostafa
Johns Hopkins School of Medicine
Jonathan B. Gubbay
University of British Columbia
Samir N. Patel
Public Health Ontario
Jianhong Wu
York University
Venkata R. Duvvuri
Venkata.Duvvuri@oahpp.ca

Public Health Ontario

Article

Keywords: Enterovirus-D68, Whole Genome Sequence Data, Case Counts, Phylodynamics, Outbreak Potential, Transmission Dynamics, Reproduction Number, Infection Duration, Infection Period

Posted Date: May 15th, 2024

DOI: https://doi.org/10.21203/rs.3.rs-4362075/v1

Additional Declarations: Competing interest reported. JBG is a paid consultant scientific editor for GIDEON Informatics, Inc., which is unrelated to the current work. HMM serves on the advisory board of Seegene, an advisor for BD Diagnostics and has research collaborations with DiaSorin and Hologic, none of these affiliations are related to the current work. Other authors have no conflicts of interest to disclose.

Abstract

Enterovirus D68 (EV-D68) has emerged as a significant cause of acute respiratory illness in children globally, notably following its extensive outbreak in North America in 2014. A recent outbreak of EV-D68 was observed in Ontario, Canada, from August to October 2022. Our phylogenetic analysis revealed a notable genetic similarity between the Ontario outbreak and a concurrent outbreak in Maryland, USA. Utilizing Bayesian phylodynamic modeling on whole genome sequences (WGS) from both outbreaks, we determined the median peak time-varying reproduction number (R_t) to be 2.70 (95% HPD 1.76, 4.08) in Ontario and 2.10 (95% HPD 1.41, 3.17) in Maryland. The R_t trends in Ontario closely matched those derived via EpiEstim using reported case numbers. Our study also provides new insights into the median infection duration of EV-D68, estimated at 7.94 days (95% HPD 4.55, 12.8) in Ontario and 10.8 days (95% HPD 5.85, 18.6) in Maryland, addressing the gap in the existing literature surrounding EV-D68's infection period. We observed that the estimated Time since the Most Recent Common Ancestor (TMRCA) and the epidemic's origin coincided with the easing of COVID-19 related social contact restrictions in both areas. This suggests that the relaxation of non-pharmaceutical interventions, initially implemented to control COVID-19, may have inadvertently facilitated the spread of EV-D68. These findings underscore the effectiveness of phylodynamic methods in public health, demonstrating their broad application from local to global scales and underscoring the critical role of pathogen genomic data in enhancing public health surveillance and outbreak characterization.

Introduction

Phylodynamic methods use pathogen genetic sequences to construct phylogenies to study the diversification of pathogens at different spatio-temporal scales, while inferring key epidemic patterns of transmission between locations[16–18]. Hodcroft et al., (2022)[12] reported key aspects of EV-D68 antigenic evolution, showing that age structure within populations has important implications for the diversification of surface proteins and host-specificity of lineages. Other phylodynamic analyses of EV-D68 have studied the relatedness between major epidemics and global circulation[11,19,20].

Non-polio enteroviruses like EV-D68 are not nationally notifiable infections in North America. As such, case documentation is low which leads to a gap in our understanding of the transmission dynamics of these viruses. For instance, information on the infection period of EV-D68 is limited. Most enterovirus infections are found to shed from the upper respiratory tract over 1 to 3 weeks[21]. A previous epidemiological modelling study of EV-D68 used an infection period of 7 days[22], which was derived from poliovirus[23,24]. Tambyah et al., (2019)[25] described EV-D68 as having 1 to 5 days of incubation period and an infectious period from 1 day before to 5 days post symptom onset but give no reference. Mild symptoms of a median duration of 6 days (range 3 to 10 days) were observed during an EV-D68 outbreak at an elder care facility[26].

In this study, we aim to address knowledge gaps on EV-D68's transmission dynamics. We investigate the evolutionary history and relatedness of EV-D68 in Ontario and on a global scale, with a specific focus on the 2022 outbreak. We provide a contextual perspective by examining the outbreak's geographical patterns within the B3 sub-clade of EV-D68 viruses. In particular, we find a high degree of genetic relatedness between samples from the 2022 outbreak, in Ontario, Canada[6] and in Maryland, United States[7,9]. We investigate the epidemic transmission (via time-varying reproduction number (R_t) estimation) through phylodynamic modelling of these two outbreaks, while shedding light on the infection duration of EV-D68 viruses. With EV-D68 reporting dates being available for the Ontario outbreak, we compare R_t as estimated via phylodynamic methods to more conventional methods (analyzing case incidence data with EpiEstim)[27]. We present epidemiological parameters derived from genome sequences, which can offer actionable information for public health practitioners.

Methods

Specimen Collection and Whole Genome Sequencing of 2022 EV-D68 in Ontario

Specimens submitted to Public Health Ontario Laboratory (PHOL) between July 31 and October 30, 2022, were collected from individuals with respiratory symptoms across various healthcare facilities in Ontario as part of routine care. EV-D68 was identified in 60.1% (n = 238) of randomly selected enterovirus-positive specimens (n = 396), with a predominant presence in nasal or nasopharyngeal samples. The highest number of EV-D68 positive test results was found among children less than 5 years of age. None of these cases presented with AFM. Additionally, whole genome sequencing was conducted on 36.5% (n = 87) of the randomly selected EV-D68 positive specimens [6].

EV-D68 WGSs were retrieved from the National Center for Biotechnology Information (NCBI) from which a consensus sequence was created. The consensus sequence used for designing three primer pairs with an overlap of ~ 600 bp spanning the entire genome (**Table S1**). Total RNA was extracted using the NucliSENS EMAG system following manufacturer's instructions (bioMérieux Canada Inc, St-Laurent, Quebec, Canada) and reverse transcribed into cDNA using LunaScript® RT SuperMix Kit (cat# M3010, New England BioLabs, Ipswich, MA, USA). The synthesized cDNAs were used as templates for amplification of 3 long overlapping fragments along the genome. Each PCR reaction of 25 µl included the following: 5 µl of Q5 Hot Start buffer (New England Biolabs, Ipswich, MA), 0.5 µl of 10 mM dNTP, 0.5 µl of Q5 High-Fidelity DNA Polymerase, 1 µL of primer mix (10µM), 2.5µL of template DNA, and 15.5 µL of PCR grade water. The following thermal cycling conditions were used on an ABI SimpliAmp thermocycler: initial denaturation at 98°C for 2 min, followed by 45 cycles at 98°C for 10 seconds and 65°C for 1 min, and a final extension at 72°C for 5 min. The presence of each PCR product was confirmed by electrophoresis on 1% agarose gel. Equimolar amounts of each PCR product from the three reactions were pooled and cleaned with AMPure XP beads (0.5 ratio) for Illumina library preparation. Paired-end libraries for the MiniSeq platform were generated using Nextera XT DNA Library Prep Kit

(Illumina) and subsequently purified using Agencourt AMPure XP beads (Beckman Coulter). The quality and size of prepared libraries were measured on the Agilent 4200 Tape Station using a High Sensitivity D1000 ScreenTape and reagent (HSD1000). Pooled normalized specimens, at a final concentration of 1.2 pM, were loaded onto a MiniSeq High Output Reagent Kit (300-cycles) and sequenced on an Illumina MiniSeq. For sequence analyses, FASTQ files were imported into CLC Genomics Workbench version 8.0.1 (CLC bio, Germantown, MD, USA). Reads were trimmed and mapped to the reference EV-D68 genome NY328 (GenBank: KP745766.1). Sequences were annotated using VAPiD v1.6.7[28] prior to their submission to GenBank.

Retrieving publicly available EV-D68 Sequence data

To perform phylogenetic analyses, additional EV-D68 sequences were obtained from the NCBI virus database at the end of May 2023. For Whole Genome Sequences (WGS) the following filters were applied to remove sequences: without sample collection date, sequences < 5000 bp in length and sequences where the proportion of nucleotides unassigned was over 0.05. Along with the WGS data produced from the Ontario 2022 outbreak (n = 87), a global dataset of 1134 EV-D68 WGSs was curated.

Phylodynamic Analysis of the 2022 EV-D68 Outbreaks in Ontario and Maryland Using Genome Sequence Data

Sequence Analysis and Phylogenetic Construction

The Nextstrain Augur v22.0.2[29] pipeline was used to align the WGS (n = 1134, length > 5000 bp) data via MAFFT v7.505[30], build a maximum likelihood (ML) phylogenetic tree via IQTree v2.0[31], and refine the tree and infer node ancestry via TreeTime v0.10.1[32]. Auspice v2.37.1[29] was used for visualization of Augur outputs. The curated 2022 outbreak WGS datasets from Ontario (ON-2022, n = 87) and Maryland (MD-2022, n = 74) were utilized in building phylodynamic models. TempEst v 1.5.1[33] was employed to check that the temporal signals in ON-2022 and MD-2022 datasets are strong enough to allow phylodynamic analyses. Both ML trees derived from the ON-2022 and the MD-2022 datasets demonstrate a strong association between genetic distances and sampling dates.

Genome-based Epidemiological Modelling using Bayesian Phylodynamics

Bayesian phylodynamic analyses were performed on the curated ON-2022 (n = 87) and MD-2022 (n = 74) EV-D68 WGS datasets. These datasets were analyzed using BEAST v2.7.5[34]. Birth-Death Skyline Serial (BDSS using BDSKY v1.5.0[35]) models were fitted to each dataset separately. We used an HKY85 site substitution model with four gamma rate categories to estimate the evolutionary rate and an optimal relaxed molecular clock model[36] that assumes heterogeneous substitution rates across phylogenetic branches, with an initial mean clock rate of 0.003[11].

Considering the possible infection periods put forward for EV-D68[21–23,25,26], we fitted all BDSS models using a prior for the infection period with a mean of 7 days and a wide standard deviation so as to cover 3 to 21 days (**Figure S1**). Birth-Death models do not estimate rate of reproductive maturation. Therefore, the model assumes patients immediately become infectious upon infection and remain infectious until being removed, i.e. there is no latent or exposed period[37]. The mean infection period (δ^{-1}) was inverted to become the death rate or rate of becoming uninfectious (δ, also called the recovery rate) and converted to years (i.e. δ = 1/7 days = 52 year^{-1}). To produce a gamma distributed prior[38] for δ, we used formulas $shape = \frac{mean^2}{variance} = 12.018$ and $scale = \frac{variance}{mean} = 4.3269$ with a standard deviation of 15 year^{-1}. All other parameter priors are listed in **Table S2.**

Three additional independent runs were performed for each model. The performance of these independent runs was evaluated using Tracer v1.7.2[39], checking the convergence of parameter, posterior, and likelihood values, along with screening individual runs ensuring effective sample sizes (ESS) > 200[40] for all parameters. We repeated the analyses until we obtained at least three model runs meeting the above convergence criteria. Log and tree files were then combined using Log Combiner v2.7.5 [40]. The bdskytools package in R (available at: https://github.com/laduplessis/bdskytools) was then used to produce skyplot figures of R_t and KDE plots of epidemic origin from the combined log files. The Python v3.10 package Seaborn v0.12.2 was used to produce box-violin plots of other parameter posterior distributions.

Mathematical Analysis of 2022 EV-D68 Outbreak in Ontario Using Case Counts Data

The package EpiEstim v 2.2-4 [27] in R v4.1.2 was employed to calculate the time varying reproduction number (R_t) from the time-series data of laboratory-confirmed positive cases of EV-D68 in Ontario during 2022. Due to the challenge in obtaining the serial interval for EV-D68, a mean serial interval of 3.7 days with a standard deviation (SD) of 2.6 days, as observed in the related pathogen EV-71[41], was used for R_t estimation via EpiEstim[25]. Considering this a sensitivity analyses was performed on the EpiEstim analyses assuming a mean serial intervals of 2 and 7 days, but keeping the same SD.

Statistical Analysis, Code Availability and GenBank Accession Numbers

The code developed in this study and the BEAUTi-created xml files are available on GitHub at Grunnill-Duvvuri-co-publications/Transmission-dynamics-inferred-from-Enterovirus-D68-genomic-data-from-2022-North-American-outbreaks (github.com). All genome sequences of the 2022 Ontario EV-D68 outbreak isolates obtained in this study were submitted to GenBank under the accession numbers PP474817 to PP474903. The 2022 Maryland EV-D68 genome sequences were obtained from GenBank (accession numbers OP321139-OP321154, OP389245-OP389246, OP572035-OP572095)[7].

Results

Phylogenetics of Ontario 2022 EV-D68 in a global epidemic context

The Ontario 2022 EV-D68 isolates cluster with concurrent specimens from Maryland 2022 [7] along with a few concurrent sequences from Sweden and France (Fig. 1). All these isolates are of the B3 sub-clade and diversify from internal node **X in** Fig. 1, which is close to a cluster of US 2018 isolates. The majority of the Ontario 2022 isolates form a sub-grouping with isolates from the Maryland 2022 outbreak and a single Swedish 2022 isolate. This sub-grouping diversifies from internal node **Y in** Fig. 1, which is close to Australian 2019 (early) isolates. A single isolate from Ontario 2022, diversifying from the internal node **Z as shown in** Fig. 1, forms a sub-grouping with sequences from Maryland 2022, Sweden 2022, France 2021–2022 and other parts of the US in 2021. Additionally, this branch, originating from the internal node that clusters with isolates from a late 2019 to early 2020 outbreak in the Netherlands.

Phylodynamic Analysis of the 2022 EV-D68 Outbreaks in Ontario and Maryland Using Genome Sequence Data

Inference of Evolutionary Parameters: Substitution Rate and Time since Most Recent Common Ancestor (TMRCA)

There are slight differences in the estimated median substitution rates between the BDSS models fitted to different datasets. The dataset ON-2022 has a median estimate of 0.0148 substitutions per site per year (95% Highest Posterior Density (HPD) 0.0112, 0.0185) and the MD-2022 dataset a median estimate of 0.0113 substitutions per site per year (95% HPD 0.00778, 0.0154). There is a higher coefficient of variation (median) of substitution rate for the MD-2022, 0.879 (95% HPD 0.706, 0.11) compared to ON-2022's 0.655 (95% 0.499, 0.838 HPD) (Fig. 2A), however the 95% HPD excludes 0 for both datasets, indicating strong support for a relaxed clock model[40]. The median TMRCA estimate for the ON-2022 dataset was February 16, 2022, with 95% HPD interval from December 26, 2021 to March 31, 2022. For the MD-2022 dataset, the median TMRCA estimate was July 11, 2021, with a 95% HPD interval from April 3, 2021 to November 3, 2021. (Fig. 2B).

Inference of Epidemiological Parameters: Infection Period, Epidemic Origin and Time-varying Reproduction number (R_t)

The estimated median duration of the infection period (in days) were 7.94, with a 95% HPD interval ranging from 4.55 to 12.8 for the Ontario outbreak, and 10.8 with 95% HPD 5.85, 18.6 for the Maryland outbreak (Fig. 3A).

The median epidemic origin estimate was February 7, 2022 (95% HPD interval, December 21, 2021, April 20, 2022) for the Ontario EV-D68 outbreak (dataset, ON-2022). The Maryland EV-D68 outbreak (MD-2022 dataset) has a median epidemic origin estimate, June 8, 2021 (95% HPD interval, March 9, 2021, September 14, 2021) (Fig. 3B). It is interesting to note that the estimates of TMRCA (Fig. 2A and Fig. 2B) of both epidemics overlapped with these origin estimates.

BDSS models estimate a rise in the time-varying reproduction number (R_t) leading to a plateaued peak occurring in the summer of 2022 (Fig. 3C), which models fitted to the Ontario dataset (ON-2022) having a higher and later but shorted peak in R_t compared to models fitted to the Maryland dataset (MD-2022). The median R_t values for these peaks are 2.70 with 95% HPD 1.76, 4.08 for the Ontario outbreak and 2.10 with 95% HPD 1.41, 3.17 for the Maryland outbreak.

Mathematical Analysis of 2022 EV-D68 Outbreak in Ontario Using Case Counts Data

Figure 4 shows that R_t estimated via case counts has a comparable peak to the R_t estimates from the phylodynamic (BDSKY) analysis of genome sequence data. Likewise, both methodologies estimate a decline in R_t from early September 2022. R_t estimates produced by BDSKY and EpiEstim are more comparable when the higher serial interval (mean 7, SD = 2.6) was used for the EpiEstim based analyses. It should be noted that the case counts are a small samples size, and no genome sequence data were obtained from clinical cases beyond October 6, 2022 (Fig. 4D).

Discussion

The phylogenetic and phylodynamic analyses reported here have demonstrated key features of two concurrent North American EV-D68 outbreaks and EV-D68's epidemiology more widely. Through phylogenetic approaches we have demonstrated the epidemiological connection between the 2022 EV-D68 outbreaks in Maryland and Ontario. Our use of phylodynamic methods have aided in narrowing down the plausible window for EV-D68's infection period. Furthermore, we have illustrated the practicality of phylodynamic methods in deriving R_t and epidemic origin. Notably, our epidemic origin estimates for the 2022 EV-D68 outbreaks coincide with the removal of restriction aimed at curtailing the spread of COVID-19.

Cross-border disease dynamics between North American countries have been studied for other viral pathogen such as SARS-CoV-2, mumps virus and West Nile viruses[42–44]. In our analysis we demonstrate close genetic proximity between viruses circulating in Maryland and Ontario in 2022, where isolates captured from each outbreak cluster within the same sub-clade, B3, and share recent common ancestry. These viruses belong to the B3 clade of EV-D68 lineages which have previously been shown to play an important role in outbreaks in the region[13,45]. The genetic proximity of these isolates indicates that significant epidemiological connections exist between these regions.

Using phylodynamic modelling we were able to estimate important epidemiological parameters: the infection period and the time-varying reproduction number (R_t). Our models showed highest support for a duration of infection of 7.94 days (95% HPD 4.55, 12.8 days) for the ON-2022 dataset (n = 87) and 10.8 days (95% HPD 5.85, 18.6 days) for the MD-2022 dataset. Prior estimates of the infection period are lacking, however, respiratory viral shedding for enteroviruses has been documented to be between 1–3 weeks[21]. Specifically, the infection period for the EV-D68 ranges from 6–10 days[25], and a symptomatic period from 3–10 days[26]. More recently Nguyen-Tran et al., (2023)[8] found that the EV-D68 genome could be detected in the upper respiratory tract for a median of 12 days post symptom onset (7–15 days). Nguyen-Tran et al., (2023)[8] point out that these RNA detection period should only be seen as an upper limit for infectious period. Given that infectious period (unlike infection period) does not include the latency period, Nguyen-Tran et al.,'s (2023)[8] findings are concurrent with our infection period of 7.94–10.8 days. The concurrence between our findings and Nguyen-Tran et al.,'s (2023)[8] brings important specificity, which is clinically relevant in the management of patients, given the previously suggested broad range in infection periods for EV-D68.

Our time-varying reproduction number (R_t) estimates derived through phylodynamic methods produced similar values compared to deriving R_t through case count data and the serial interval (Fig. 4). Of particular note, greater concordance was seen when case count derived R_t values used a higher serial interval (mean = 7 days, SD = 2.6). Our mid-point serial interval for EV-D68 (mean = 3.6 days, SD = 2.6) was based on EV-71[41], but given our estimate of the EV-D68 infection period (7.94–10.8 days) and an upper limit for the infectious period of 12 days[8], EV-D68's serial interval is likely to be closer to the higher value used in our sensitivity analysis. Previous epidemiological estimates of R_t from EV-D68 outbreaks (across several US states 2014-17) range between 0.5-1.6[22]. We find that our estimates of the median R_t (Fig. 4) were just over 1 in non-epidemic periods and 2.70 (95% HPD 1.76, 4.08) in Ontario and 2.10 (95% HPD 1.41, 3.17) in Maryland during the respective peak epidemic periods. A build up in the susceptible population due to reduced contacts over 2020–2021 may have led to the increased R_t values observed in Ontario and Maryland 2022, compared to estimates from several US states over 2014-17, a pre-pandemic period[22]. More generally, our EV-D68 BDSKY derived R_t estimates are consistent with other respiratory pathogens particularly other enteroviruses[24,46–49]. As with Park et al., (2021) [22], we found delays in the increase of R_t were associated with outbreaks occurring farther north within North America.

The WGS-based substitution rates reported here, 0.0148 substitution per site per year (95% HPD 0.0112, 0.0185) for ON-2022 and 0.0113 substitution per site per year (95% HPD 0.0078, 0.0154) for MD-2022, are substantially higher than reported previously, 0.003 substitution per site per year[11]. The 38 WGS used in the analysis Eshaghi et al., (2017) [11] come from 14 different countries, span 1960–2014 and therefore come from different EV-D68 clades, whereas, the WGS being used in our analyses are from one regional outbreak of a single sub-clade, B3. Time varying evolutionary metrics have been observed before, with faster rates observed when samples are drawn from shorter time periods[50–52]. Ghafari et al., (2022)[53] demonstrated that during the SARS-CoV-2 and pH1N1 influenza pandemics this time varying

evolutionary rate could be attributed to a short-term buildup of mildly deleterious mutations, that were eradicated over a longer term through purifying selection. This process of incomplete purifying selection may be the reason for the discrepancy between the EV-D68 substitution rates reported here and earlier[11].

The estimated 2022 EV-D68 epidemic origin and TMRCA statistics from BDSS models for both regions coincide with the periods when measures to reduce social contact, known as Non-Pharmaceutical Interventions (NPIs), were relaxed. Specifically, in Ontario, Canada, the period was from January 31, 2022 to March 14, 2022, coinciding with the decline of the Omicron COVID-19 wave[54]. Meanwhile, the Maryland data corresponded with the phase of winding down several NPIs aimed at curtailing the spread of COVID-19, from early February 2021 to August 13, 2021[55–57]. NPIs aimed at controlling COVID-19 transmission have also significantly reduced influenza cases, virtually eliminated respiratory syncytial virus (RSV) hospitalization and diminish detectable circulation of several enteroviruses[58–61]. Therefore, it is possible that the coinciding of our epidemic origin and TMRCA estimates with the lifting of NPIs demonstrates the suppressing effect of NPIs on EV-D68 transmission. However, Fig. 1 depicts 2022 EV-D68 Maryland and Ontario sequences interspersed with each other and sequences from Sweden. This pattern suggests that the 2022 EV-D68 outbreaks in Ontario and Maryland may be the result of several independent introductions into their respective populations, and not a single introduction. This would mean that our R_t estimates are more likely to be for EV-D68 outbreaks in regions greater than Ontario or Maryland the further back in time the estimate is. Likewise, this may mean that our TMRCA and origin estimates are for EV-D68 outbreaks occurring over a much wider region than Ontario or Maryland.

This study has limitations that should be addressed in further research efforts. For instance, the above caveats over R_t, TMRCA and origin estimates have, in part, come about through sampling in acute healthcare settings during an ongoing transmission within the wider community (Fig. 4C). It is important that sampling efforts are broader and capture more localities nationally, as well as broadly in North America, if not globally. As seen in the wider phylogenetic analysis (Fig. 1) there are long branches across the phylogeny which may indicate prolonged periods of within-host evolution, missed infections or un-sampled diversity. Thus, active surveillance is critical in identifying major source and sink populations for the EV-D68 virus, directing intervention efforts effectively. In addition to sampling biases, it is important that clinical observation studies of positive cases are conducted to validate the in-silico estimates of infection period for EV-D68 viruses to robustly model epidemiological dynamics further.

Future study of EV-D68 in a phylodynamic framework will not only be bolstered by wider sampling efforts but will also be aided by the inclusion of secondary metadata to study the importance of different host traits on viral evolution and diffusion. If metadata pertaining to severity of infection, age, and travel history of a patient is available phylodynamic methods can be used to determine the importance of traits in the diffusion process and potentially identify host characteristics that can inform control measures[62,63]. In summary, this study underscores the importance of pathogen genome surveillance combined with phylodynamics in complementing conventional epidemiological approaches within public health investigations.

Declarations

Author contributions

Conceptualization: M.G and V.R.D., methodology: M.G., A.E., S.N., A.P., A.G., C.C., V.R.D., formal analysis: M.G., A.E., P.B., and A.G, funding acquisition: J.W. and V.R.D, investigation: M.G., and A.E., supervision: V.R.D, validation: L.D., A.G., L.D.P., V.R.D, visualization: M.G., writing - original draft preparation: M.G., writing – review & editing: A.E., L.D., S.N., A.G., T.B., S.C., A.P., S.I., P.B., L.D.P., C.L.M., C.C., S.M., M.H, J.B., H.H.M., J.B.G., S.N.P., J.W., and V.R.D.

Acknowledgements

We acknowledge the authors, originating and submitting laboratories of the sequences from NCBI Database on which this research is based. MG and JW were supported by the NSERC-PHAC Emerging Infectious Disease Modeling Initiative Mathematics for Public Health. MG received The Emerging and Pandemic Infections Consortium (EPIC) 2023 researcher mobility award to participate in the 'Taming the Beast" workshop at Squamish, British Columbia, Canada.

Conflict of Interest

JBG is a paid consultant scientific editor for GIDEON Informatics, Inc., which is unrelated to the current work. Other authors have no conflicts of interest to disclose.

Ethics Statement

This project has received ethics review clearance from Public Health Ontario's Ethics Review Board.

References

1. Schieble, J. H., Fox, V. L. & Lennette, E. H. A probable new human picornavirus associated with respiratory disease. American Journal of Epidemiology 85, 297–310 (1967).
2. Levy, A. *et al.* Enterovirus D68 disease and molecular epidemiology in Australia. Journal of Clinical Virology 69, 117–121 (2015).
3. Messacar, K. *et al.* Enterovirus D68 and acute flaccid myelitis—evaluating the evidence for causality. The Lancet Infectious Diseases 18, e239–e247 (2018).
4. Kramer, R. *et al.* Molecular diversity and biennial circulation of enterovirus D68: A systematic screening study in Lyon, France, 2010 to 2016. Eurosurveillance 23, 1700711 (2018).
5. Gilrane, V. L. *et al.* Biennial upsurge and molecular epidemiology of enterovirus D68 infection in New York, USA, 2014 to 2018. Journal of Clinical Microbiology 58, (2020).

6. Public Health Ontario. *Surveillance Report: Enterovirus D68 Testing at Public Health Ontario.* 1–6 (2022).
7. Fall, A. *et al.* An increase in enterovirus D68 circulation and viral evolution during a period of increased influenza like illness, The Johns Hopkins Health System, USA, 2022. Journal of Clinical Virology 160, 105379 (2023).
8. Nguyen-Tran, H. *et al.* Duration of Enterovirus D68 RNA Shedding in the Upper Respiratory Tract and Transmission among Household Contacts, Colorado, USA. Emerging Infectious Diseases 29, 2315–2324 (2023).
9. Fall, A. *et al.* Circulation of Enterovirus D68 during Period of Increased Influenza-Like Illness, Maryland, USA, 2021. Emerg Infect Dis 28, 1525–1527 (2022).
10. ICTV. ICTV. Enterovirus D Taxon Details. https://ictv.global/taxonomy/taxondetails?taxnode_id=202201986 (2021).
11. Eshaghi, A. *et al.* Global distribution and evolutionary history of enterovirus D68, with emphasis on the 2014 outbreak in Ontario, Canada (Supplementary Material). Frontiers in Microbiology 8, 257 (2017).
12. Hodcroft, E. B. *et al.* Evolution, geographic spreading, and demographic distribution of Enterovirus D68. PLoS Pathog 18, e1010515 (2022).
13. Wang, G. *et al.* Enterovirus D68 Subclade B3 Strain Circulating and Causing an Outbreak in the United States in 2016. *Scientific Reports 2017 7:1* 7, 1–8 (2017).
14. Piralla, A. *et al.* Enterovirus-D68 (EV-D68) in pediatric patients with respiratory infection: The circulation of a new B3 clade in Italy. Journal of Clinical Virology 99–100, 91–96 (2018).
15. Midgley, S. E. *et al.* Co-circulation of multiple enterovirus D68 subclades, including a novel B3 cluster, across Europe in a season of expected low prevalence, 2019/20. Euro Surveill 25, 1900749 (2020).
16. Duvvuri, V. R. *et al.* Comparing the transmission potential from sequence and surveillance data of 2009 North American influenza pandemic waves. Infectious Disease Modelling 8, 240–252 (2023).
17. Volz, E. M., Koelle, K. & Bedford, T. Viral Phylodynamics. PLoS Computational Biology 9, e1002947 (2013).
18. Baele, G., Suchard, M. A., Rambaut, A. & Lemey, P. Emerging concepts of data integration in pathogen phylodynamics. in *Systematic Biology* vol. 66 e47–e65 (Oxford Academic, 2017).
19. Tan, Y. *et al.* Molecular Evolution and Intraclade Recombination of Enterovirus D68 during the 2014 Outbreak in the United States. J Virol 90, 1997–2007 (2016).
20. Simoes, M. P. *et al.* Epidemiological and clinical insights into the enterovirus D68 upsurge in Europe 2021/22 and the emergence of novel B3-derived lineages, ENPEN multicentre study. J Infect Dis jiae154 (2024) doi:10.1093/infdis/jiae154.
21. Messacar, K. & Abzug, M. J. Enteroviruses and Parechoviruses. in *Principles and Practice of Pediatric Infectious Diseases* 1228–1236.e3 (Elsevier, 2023). doi:10.1016/b978-0-323-75608-2.00236-6.

22. Park, S. W. *et al.* Epidemiological dynamics of enterovirus D68 in the United States and implications for acute flaccid myelitis. Science Translational Medicine 13, 1–14 (2021).
23. Casey, A. E. OBSERVATIONS ON AN EPIDEMIC OF POLIOMYELITIS. Science 95, 359–360 (1942).
24. Pons-Salort, M. & Grassly, N. C. Serotype-specific immunity explains the incidence of diseases caused by human enteroviruses. Science 361, 800–803 (2018).
25. Tambyah, P., Isa, M. S. & Tan, C. X. T. New and Emerging Infections of the Lung. in *Kendig's Disorders of the Respiratory Tract in Children* 466–474.e2 (Elsevier, 2019). doi:10.1016/B978-0-323-44887-1.00028-6.
26. Bal, A. *et al.* Enterovirus D68 nosocomial outbreak in elderly people, France, 2014. Clinical Microbiology and Infection 21, e61–e62 (2015).
27. Cori, A., Ferguson, N. M., Fraser, C. & Cauchemez, S. A new framework and software to estimate time-varying reproduction numbers during epidemics. American Journal of Epidemiology 178, 1505–1512 (2013).
28. Shean, R. C., Makhsous, N., Stoddard, G. D., Lin, M. J. & Greninger, A. L. VAPiD: a lightweight cross-platform viral annotation pipeline and identification tool to facilitate virus genome submissions to NCBI GenBank. BMC bioinformatics 20, 1–8 (2019).
29. Hadfield, J. *et al.* NextStrain: Real-time tracking of pathogen evolution. Bioinformatics 34, 4121–4123 (2018).
30. Katoh, K. & Standley, D. M. MAFFT multiple sequence alignment software version 7: Improvements in performance and usability. Molecular Biology and Evolution 30, 772–780 (2013).
31. Minh, B. Q. *et al.* IQ-TREE 2: New Models and Efficient Methods for Phylogenetic Inference in the Genomic Era. Molecular Biology and Evolution 37, 1530–1534 (2020).
32. Sagulenko, P., Puller, V. & Neher, R. A. TreeTime: Maximum-likelihood phylodynamic analysis. Virus Evolution 4, (2018).
33. Rambaut, A., Lam, T. T., Carvalho, L. M. & Pybus, O. G. Exploring the temporal structure of heterochronous sequences using TempEst (formerly Path-O-Gen). Virus Evolution 2, (2016).
34. Bouckaert, R. *et al.* BEAST 2.5: An advanced software platform for Bayesian evolutionary analysis. PLoS Comput Biol 15, e1006650 (2019).
35. Stadler, T., Kühnert, D., Bonhoeffer, S. & Drummond, A. J. Birth-death skyline plot reveals temporal changes of epidemic spread in HIV and hepatitis C virus (HCV). Proc Natl Acad Sci U S A 110, 228–233 (2013).
36. Douglas, J., Zhang, R. & Bouckaert, R. Adaptive dating and fast proposals: Revisiting the phylogenetic relaxed clock model (Supplementary Material). PLoS Computational Biology 17, e1008322 (2021).
37. Stadler, T., Kühnert, D., Rasmussen, D. A. & Plessis, L. du. Insights into the Early Epidemic Spread of Ebola in Sierra Leone Provided by Viral Sequence Data. PLoS Curr (2014) doi:10.1371/currents.outbreaks.02bc6d927ecee7bbd33532ec8ba6a25f.

38. Bolker, B. M. *Ecological Models and Data in R*. (Princeton University Press, 2008).
39. Rambaut, A., Drummond, A. J., Xie, D., Baele, G. & Suchard, M. A. Posterior summarization in Bayesian phylogenetics using Tracer 1.7. *Systematic biology* 67, 901–904 (2018).
40. Drummond, A. J. & Bouckaert, R. R. *Bayesian Evolutionary Analysis with BEAST*. (Cambridge University Press, 2015).
41. Chang, L. Y. *et al.* Transmission and Clinical Features of Enterovirus 71 Infections in Household Contacts in Taiwan. JAMA 291, 222–227 (2004).
42. Stapleton, P. J. *et al.* Evaluating the use of whole genome sequencing for the investigation of a large mumps outbreak in Ontario, Canada. Scientific Reports 9, (2019).
43. Mann, B. R., McMullen, A. R., Guzman, H., Tesh, R. B. & Barrett, A. D. T. Dynamic transmission of West Nile virus across the United States-Mexican border. Virology 436, 75–80 (2013).
44. Murall, C. L. *et al.* A small number of early introductions seeded widespread transmission of SARS-CoV-2 in Québec, Canada. Genome Medicine 13, 1–17 (2021).
45. Uprety, P. *et al.* Association of enterovirus D68 with acute flaccid myelitis, Philadelphia, Pennsylvania, USA, 2009–2018. Emerging Infectious Diseases 25, 1676–1682 (2019).
46. Ma, E. *et al.* Estimation of the basic reproduction number of enterovirus 71 and coxsackievirus A16 in hand, foot, and mouth disease outbreaks. Pediatric Infectious Disease Journal 30, 675–679 (2011).
47. Biggerstaff, M., Cauchemez, S., Reed, C., Gambhir, M. & Finelli, L. Estimates of the reproduction number for seasonal, pandemic, and zoonotic influenza: A systematic review of the literature. BMC Infectious Diseases 14, 1–20 (2014).
48. Lim, C. T. K., Jiang, L., Ma, S., James, L. & Ang, L. W. Basic reproduction number of coxsackievirus type A6 and A16 and enterovirus 71: Estimates from outbreaks of hand, foot and mouth disease in Singapore, a tropical city-state. Epidemiology and Infection 144, 1028–1034 (2016).
49. Liu, Q. H. *et al.* Measurability of the epidemic reproduction number in data-driven contact networks. Proceedings of the National Academy of Sciences of the United States of America 115, 12680–12685 (2018).
50. Meyer, A. G., Spielman, S. J., Bedford, T. & Wilke, C. O. Time dependence of evolutionary metrics during the 2009 pandemic influenza virus outbreak. Virus Evolution 1, 1–10 (2015).
51. Aiewsakun, P. & Katzourakis, A. Time dependency of foamy virus evolutionary rate estimates. BMC Evolutionary Biology 15, 1–15 (2015).
52. Membrebe, J. V. *et al.* Bayesian Inference of Evolutionary Histories under Time-Dependent Substitution Rates. Molecular Biology and Evolution 36, 1793–1803 (2019).
53. Ghafari, M. *et al.* Purifying Selection Determines the Short-Term Time Dependency of Evolutionary Rates in SARS-CoV-2 and pH1N1 Influenza. Molecular Biology and Evolution 39, 1–8 (2022).
54. Government of Ontario. Ontario Outlines Steps to Cautiously and Gradually Ease Public Health Measures. *NEWS RELEASE* https://news.ontario.ca/en/release/1001451/ontario-outlines-steps-to-

cautiously-and-gradually-ease-public-health-measures (2022).

55. Neives, R., O'Brien, M., Shipley, J., Green, K. & Laping, S. *Summary of State-Specific Government Response to COVID-19 in the US 2020/2021 - MARYLAND*. 1–15 (2023).
56. Ng, G., Fulginiti, J. & Lucas, T. 2021 Timeline: Coronavirus in Maryland. *WBalTV* https://www.wbaltv.com/article/covid-19-in-maryland-2021-timeline/35169408 (2022).
57. Lucas, T., Young, B. & Ng, G. 2022 Timeline: Coronavirus in Maryland. *WBalTV* https://www.wbaltv.com/article/covid-19-maryland-2022-timeline/38665369 (2022).
58. Baker, R. E. *et al.* The impact of COVID-19 nonpharmaceutical interventions on the future dynamics of endemic infections. Proceedings of the National Academy of Sciences of the United States of America 117, 30547–30553 (2020).
59. Feng, L. *et al.* Impact of COVID-19 outbreaks and interventions on influenza in China and the United States. Nature Communications 12, 1–8 (2021).
60. Van Brusselen, D. *et al.* Bronchiolitis in COVID-19 times: a nearly absent disease? European Journal of Pediatrics 180, 1969–1973 (2021).
61. Forero, E. L. *et al.* Changes in enterovirus epidemiology after easing of lockdown measures. Journal of Clinical Virology 169, 105617 (2023).
62. Lemey, P., Rambaut, A., Drummond, A. J. & Suchard, M. A. Bayesian phylogeography finds its roots. PLoS Computational Biology 5, e1000520 (2009).
63. Lemey, P. *et al.* Accommodating individual travel history and unsampled diversity in Bayesian phylogeographic inference of SARS-CoV-2. Nature Communications 11, 1–14 (2020).

Figures

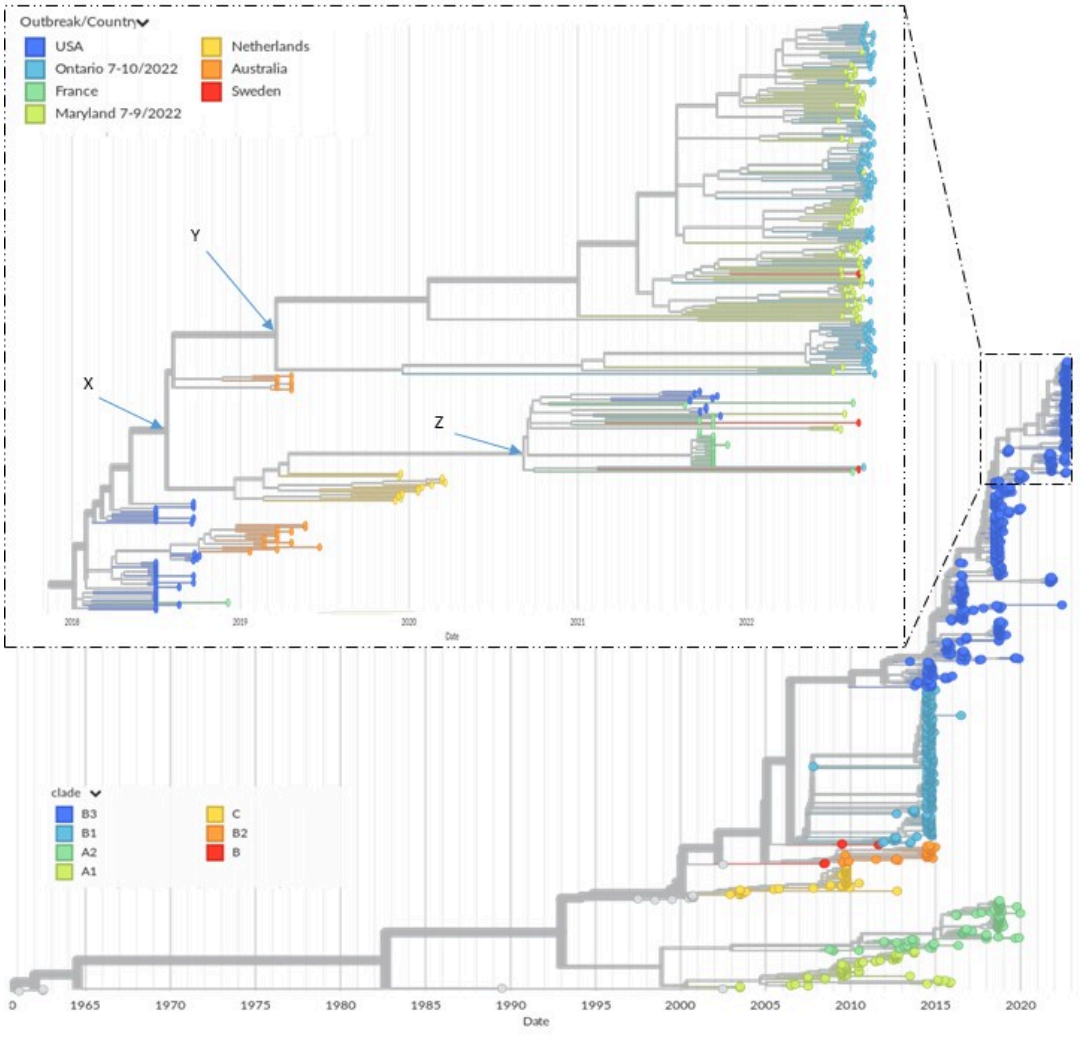

Figure 1

EV-D68 WGS based phylogenetic tree using Nextstrain[29]. The exert zooms on the 2022 EV-D68 outbreaks of Ontario, Canada and Maryland[7,9]. X, Y and Z are internal nodes of the tree referenced in the main text.

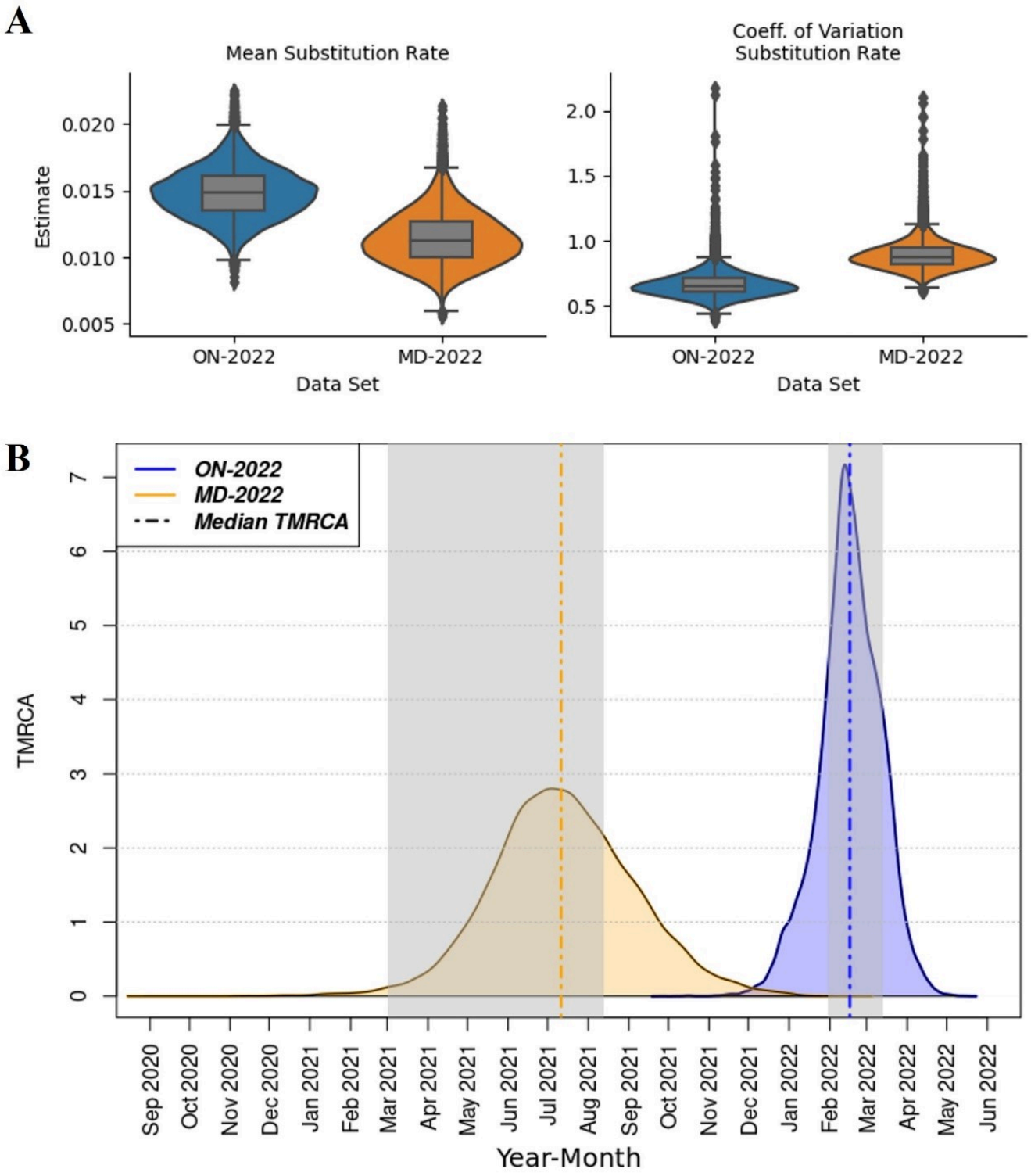

Figure 2

Distribution of posterior estimates of evolutionary parameters from 3 convergent runs of the best supported BDSS models fitted to different datasets of EV-D68 samples. A: Box-Violin plots of posterior estimates of mean and the coefficient of variation for substitution rate (per site per year). B: Kernel Density Estimate (KDE) plots of posterior estimates for TMRCA. The grey patches denote easing of COVID-19 restrictions in Maryland[55–57] on the left and Ontario[54] on the right. ON-2022 dataset contains

all WGS sequences collected from Ontario 2022 EV-D68 cases. MD-2022 dataset contains WGS sequences collected from Maryland 2022 EV-D68 cases.

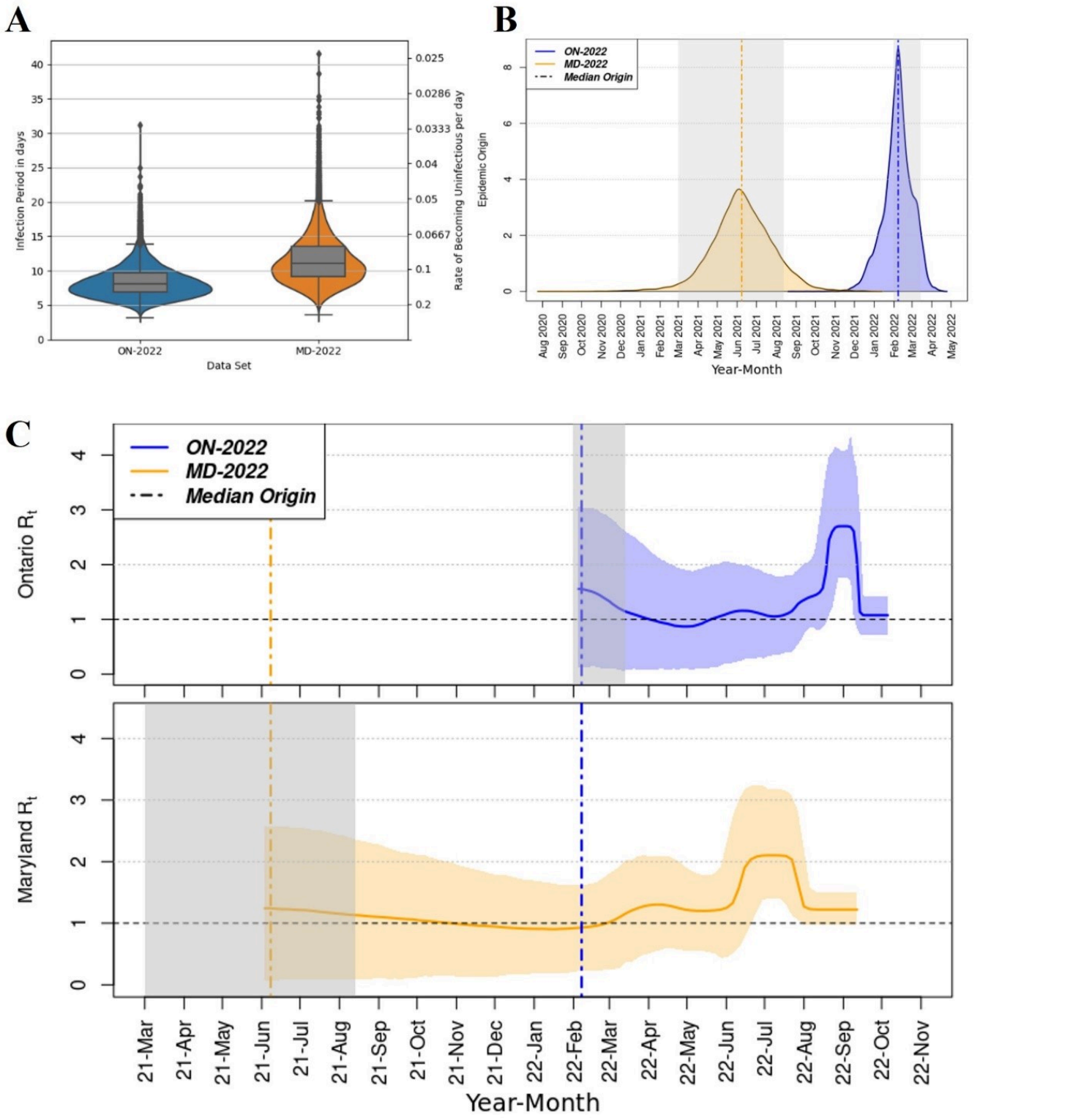

Figure 3

Distribution of posterior estimates of epidemiological parameters from 3 convergent runs of the best supported BDSS models fitted to different datasets of EV-D68 samples. A. Box-Violin plots of posterior estimates of Infection period (Rates of Becoming non-infectious). **B.** Kernel density estimate of

estimated Epidemic Origin. **C top**: R_t estimates & 95% HPD intervals for ON-2022. **C bottom**: R_t estimates & 95% HPD intervals for MD-2022. The grey patches in **B** and **C** denote easing of COVID-19 restrictions in Maryland[55–57] on the left and Ontario[54] on the right.. ON-2022 dataset contains all WGS sequences collected from Ontario 2022 EV-D68 cases. MD-2022 dataset contains WGS sequences collected from Maryland 2022 EV-D68 cases.

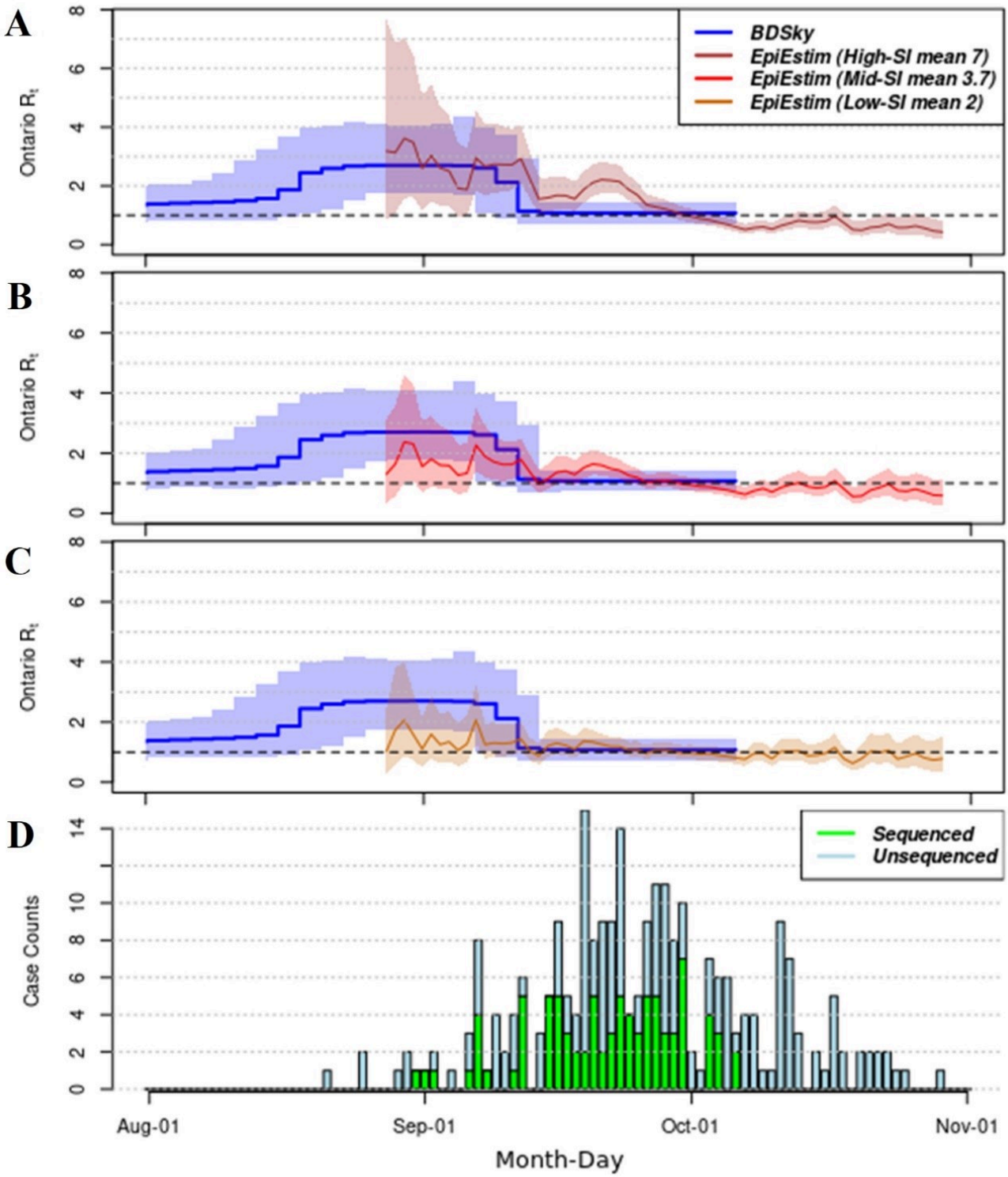

Figure 4

Comparison of Time-varying Reproduction Number (R_t) estimation from BDSKY (using genome sequence data) and EpiEstim (using case counts) methods, using Ontario 2022 EV-D68 data. Subplots A, B and C: Effective reproductive number estimated via three convergent runs of the best supported BDSS models fitted to the ON-2022 EV-D68 WGSs (blue) compared to estimation via EpiEstim case counts. All serial intervals (SI) used in EpiEstim method's had an standard deviation (SD) of 2.6, The **subplot D** depicts Ontario EV-D68 case counts used in effective reproductive number estimation, only sequenced cases in green were used in the BDSKY based method. Note the BDSKY estimate of R_t goes back until February 2022 (**Figure 3C**).

Supplementary Files

This is a list of supplementary files associated with this preprint. Click to download.

- Grunnilletal.EVD68manuscriptsupplementarymaterials.docx